High-Resolution Seismic Reflection Survey of Young Sediment at Can Gio Coast, Ho Chi Minh City, Vietnam

Thuan Van Nguyen, Cuong Van Anh Le, and Man Ba Duong

Abstract Young river sediment layers and seabed can be investigated by application of high-resolution seismic method supplied with a sub-bottom profiler. Contrast between different acoustic impedance leads to reflection of seismic waveform propagation that can image the interest geological targets. Soai Rap River is one of the two most important water gates in Ho Chi Minh city, Vietnam to the outside world. Studying its seabed and young sedimentology plays a vital in developing transportation and sea-ward economic Vietnamese policy. We have collected, processed, and interpreted ten of 2D high-resolution seismic profiles and two prior drill holes in the survey area, Can Gio district, Ho Chi Minh city. Its 3D seabed and 3D Holocene shallow sediment representations are interpolated different 2D boundaries which can be achieved by analysis of conventionally processed seismic data and seismic textural attributes (i.e., energy and entropy). Four resulted layers consists of water and young Holocene sediments and one trough channel in the middle of the river can be interpreted.

Keywords High-resolution seismic · Holocene · Bathymetry

1 Introduction

High frequency reflection seismic data has been used for researching formations of young river sediment, lowland, and seabed visualization [1–3]. Seismic waves

T. Van Nguyen · C. Van Anh Le (✉)
University of Science, Ho Chi Minh City, Vietnam
e-mail: lvacuong@hcmus.edu.vn

T. Van Nguyen
e-mail: nvthuan@hcmus.edu.vn

Vietnam National University Ho Chi Minh City, Ho Chi Minh City, Vietnam

M. B. Duong
Ho Chi Minh City Institute of Resources Geography, VAST, Ho Chi Minh City, Vietnam
e-mail: dbman@hcmig.vast.vn

L. Q. Nguyen et al. (eds.), *Advances in Geospatial Technology in Mining and Earth Sciences*, Environmental Science and Engineering,
https://doi.org/10.1007/978-3-031-20463-0_21

emitted from a sub-bottom profiler can propagate through its surrounding environment and reflect to its receiver after hitting seismic boundaries of different acoustic impedance zones [4]. With its smaller energy rather than other explosion traditional sources (i.e., air guns), the interest depth of this high-resolution seismic method can only go to hundreds of meters below the water surface. Data processing/analyzing stages can convert the raw measured data into interpretable data [5].

Our work focusses on collecting, processing, and interpreting ten 2D high-resolution seismic profiles to image seabed and young sediment at the fork area of Soai Rap River, Can Gio coast, Ho Chi Minh City, Vietnam. We have applied 3D visualization of their processed data in supporting analyzing stages. Interpreted seismic results are supported with information of two nearby drill holes. The drill holes' locations are in Thanh An island, Can Gio District [4].

2 Study Area

The acquisition area is the fork of Soai Rap River, Can Gio district, Ho Chi Minh city, Vietnam shown in Fig. 1. Known as a coastal area, Can Gio district plays a vital role in the economic development of the city when it has many important rivers connecting to the outside world. Its Soai Rap river is the second maritime route (the other is Long Tau river) for domestic and international large ships to transport imported and imported products to seaports in Ho Chi Minh city [6].

Recognized by UNESCO in 2000 as the first Mangrove Biosphere Reserve in Vietnam for having the highest diversity of mangrove living species, Can Gio also plays as "green lungs" of the city. Can Gio formed around 7000–6000 cal BP [8, 9] thanks to the Saigon-Dong Nai river basin. The factors such as semi-diurnal regime tidal from the estuary and average water discharge from Soai Rap and Long Tau rivers in the rainy season can form sand bars locating in front of their estuaries and Can Gio foreshore [4, 10].

Soai Rap river, an outlet of the Sai Gon–Dong Nai river, received a much smaller discharge of sediment compared to the Mekong River basin [11]. It is also close to the Mekong River delta. Therefore, knowledge of sediment of research area can be beneficial from geology of the Mekong delta basin and Ho Chi Minh city [4, 10, 12–17]. In Ho Chi Minh City, its northern part gets the higher elevation which are occupied by the pre–Holocene Cenozoic materials [18, 19]. Holocene sediment formations are seen in its southern areas as Nha Be and Can Gio districts [18, 19]. Investigations show that Holocene sediment patterns are linked to Sai Gon–Dong Nai river systems [18, 19]. Different acoustics impedances of types of young sediments can inspire application of high-resolution seismic method to image seabed and lowland topography [4, 5].

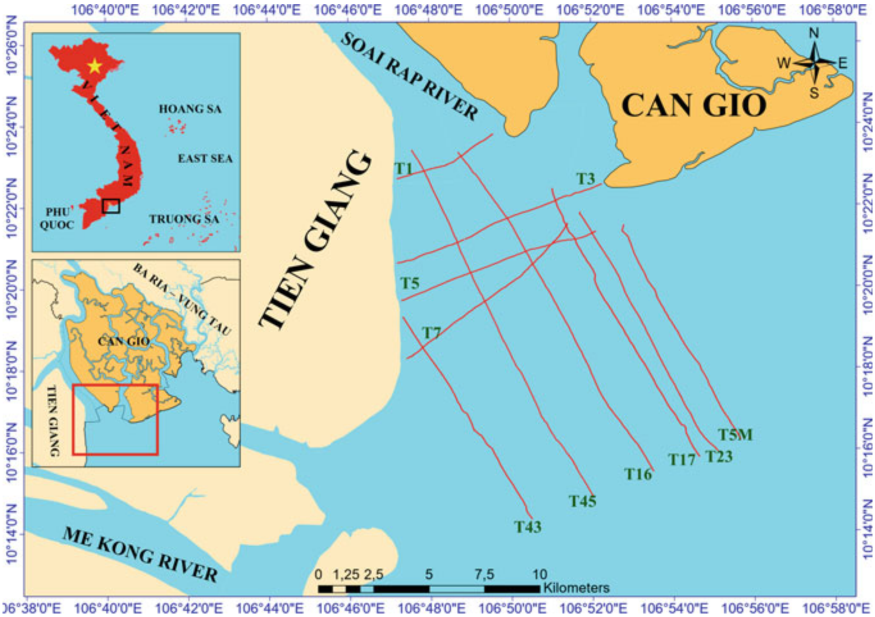

Fig. 1 Location of the survey area in Soai Rap river, Ho Chi Minh City, Vietnam [7]

3 Methodology

High-resolution seismic method is applied in searching subsurface image of maritime areas and young sediment structures thanks to wave reflections from boundaries of different acoustic impedance layers [2, 4, 20, 21].

In our research, the sub-bottom profiler, namely, SB-216S [22], typed with fixed transmitter–receiver offset is carried in a ship for data collection. Being laid 1.5 m underwater, it emits signals of the frequency range from 2 to 16 kHz in each 20 ms length which propagate through water and sediment environments [22]. During data collection stage, the ship can be detected by the GPS locator equipment while the professional software, Edge Tech Discover [23], helps to visualize the reflection seismic waves seen as electric signals in the computer monitor. In 2017, ten 2D profiles were collected in the research area, ranging from 5500 m to around 12000 m. In Fig. 2, one example shows that how the equipment is laid in the ship and seismic waves propagate through surrounding environment.

Data formats depend on data analysis/processing stages. For data collection, its seismic data format is binary with the extension *.jsf [25]. For processing/ analyzing the uninterpretable raw data to interpretable ones, we have used three professional software, Reflexw [26], OpendTect [27], and MATLAB codes [4].

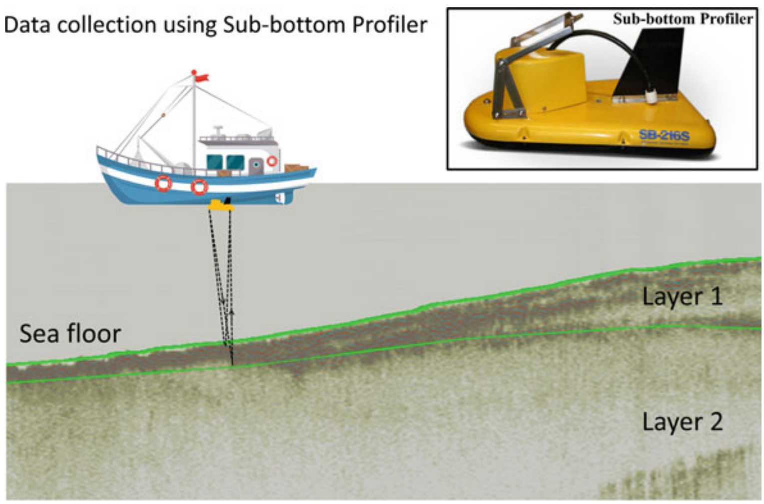

Fig. 2 Deployment of the sub-bottom profiler (SBS-216S) [4, 22, 24]. Boundary of two different acoustic impedance layers (i.e., water and sand) can be interpreted as green lines

3.1 Data Processing

Interpretable seismic data can be achieved via processing stages (Fig. 3). The first stage focuses on using processing tools in Reflexw for having interpretable seismic data in 2D view while the other stage utilizes the application of OpendTect for interpreting all the 2D data in 3D visualization.

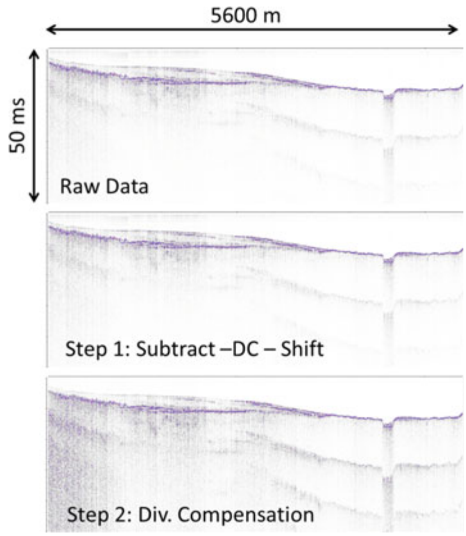

Fig. 3 Processing steps for the raw seismic data (top image) in the profile T1 [4]. Suitable amplitude gains in Divergent Compensation applied to the Step 1 processed data (middle image) can make the Step 2 processed data (bottom image) visible in the larger travel time

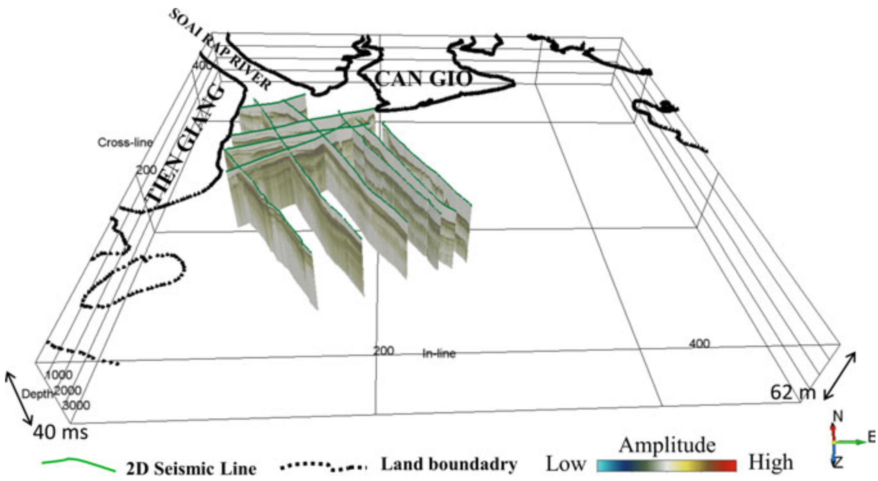

Fig. 4 Survey setting for the area. All the ten seismic profiles are put in 3D visualization. They will be input for further seismic attributes calculation

In the first stage, we applied two steps as Substract-DC-shift and Divergent (div.) Compensation Gain for all the ten seismic lines [4, 26]. A time constant shift is removed for each trace in Substract-DC-Shift filter. The Compensation Gain filter plays a vital role in reimbursing spherical energy loss while the waves propagate deeper [26].

Figure 3 illustrates one example of our first seismic processing stage for the profile T1. In the deeper part, a visible amplitude difference can be seen between two images, the raw data (top image) and the final processed image (bottom image).

In the second stage, with the help of OpendTech software, three main works are listed:

(i) 3D visualization of all the 2D processed seismic lines resulted from the first stage (Fig. 4)
(ii) validating the data quality (Fig. 5)
(iii) computation of their different seismic attributes, 3D interpolated horizons, and the Holocene layer thickness.

Coordinates of all the seismic data profiles are used to form survey settings in OpendTect platform (Fig. 4). Validating the seismic quality could be done using the technique of checking a meeting point of any two different seismic profiles [4]. In Fig. 5, all the meeting points defined from couples of two cross different seismic lines are illustrated. That is, their similar depths of their meeting points can prove high reliability of the seismic quality in terms of data measurement and analysis.

Seismic Textural Attributes: Reflectors can be recognized from extreme values of processed seismic data and its seismic attributes [4, 5, 28, 29]. We have used application of entropy and energy textural attributes to help interpretation of the main seismic reflection.

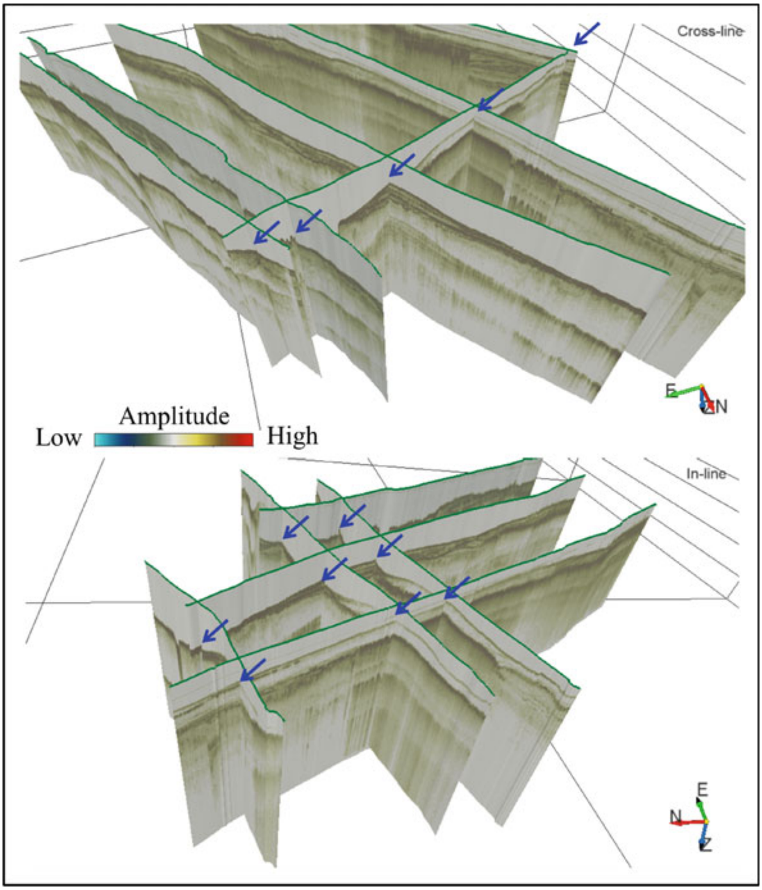

Fig. 5 Validity check of seismic data in depth analysis of the meeting points in their seismic profiles. In the meeting points, their depths of any two cross profiles should be similar. Two images (top and bottom) show the checking in different 3D view. Blue arrows refer locations of meeting points

Definition of textural attributes as energy, entropy, contrast, and homogeneity are well-known relating to detecting “zones of common signal character” [30]. The gray-level co-occurrence Matrix (GLCM) [31, 32] is established from seismic processed input data, then seismic textural attribute output such as energy or entropy are calculated from the GLCM data by the equations below[5]:

$$\text{Energy} = \sqrt{\sum_{i,j=0}^{N-1} P_{i,j}^{2}} \tag{1}$$

$$\text{Entropy} = \sum_{i,j=0}^{N-1} P_{i,j}\left(-\ln\left(P_{i,j}\right)\right) \tag{2}$$

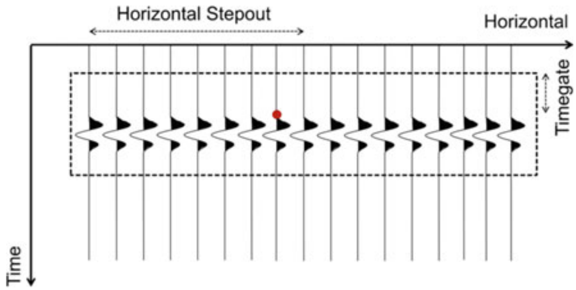

Fig. 6 Representation of 2D sliding window for computing seismic textural attributes [4, 27]. The sliding window is seen as a dashed rectangular characterizing horizontal width and time length

where $P_{i,j}$, shows the *i*th row and *j*th column of the GLCM matrix *P*.

The energy one brightens areas of high textural stability in each calculation zone which can be continuous features. The term, "Entropy" express how large randomness in the calculation zone is.

A calculation zone, namely a sliding window is characteristic through horizontal width and time length (see Fig. 6). For our research, we use time length as 2×27 ms and horizontal width as 2×9 traces.

4 Results and Discussion

We have interpreted some reflectors in the interest area. Using distinguished waveforms of processed seismic data and its seismic textural attributes (i.e., energy and entropy), three manually extracted boundaries can form three shallow layers as (i) water body, (ii) mixture of mud, sand, and silk clays layers (Present), (iii) sand silk clay sediments (Holocene), and hard gray sediment (Pleistocene).

The water body is easily recognized from strong seismic data and extreme values of its textural seismic attributes (see Fig. 7). In the Fig. 7, processed seismic data and its seismic attributes are shown for providing different view of a geology object. For example, water body can be seen as the space bounded by the surface to strong reflection boundary (see wheat color line in Fig. 7) while zone of low value for energy texture and zone of high value for entropy are represented for the water body.

Thanks to the seismic data attributes, we have interpreted different 2D seismic boundaries to form the three shallow layers. For illustrating all the 2D boundaries in 3D visualization, Fig. 8 refers seabed, top and bottom of Holocene layer as green, wheat, and pink colors, respectively. The well match in depth between of any two intersect lines can prove high correctness in seismic interpretation.

3D surfaces are interpolated from the 2D seismic boundaries (Figs. 9 and 10). We have used the Matlab built-in function, scatteredInterpolant.m [33] to build up the surfaces. 3D seabed is firstly interpreted and interpolated from strong visible reflection seismic amplitude events (Fig. 9). For the Top and Bottom interfaces of the Holocene layer, it is not consistent for strong reflection to interpret. Then, we used the visible patterns of the Holocene layer in textural seismic attributes (see

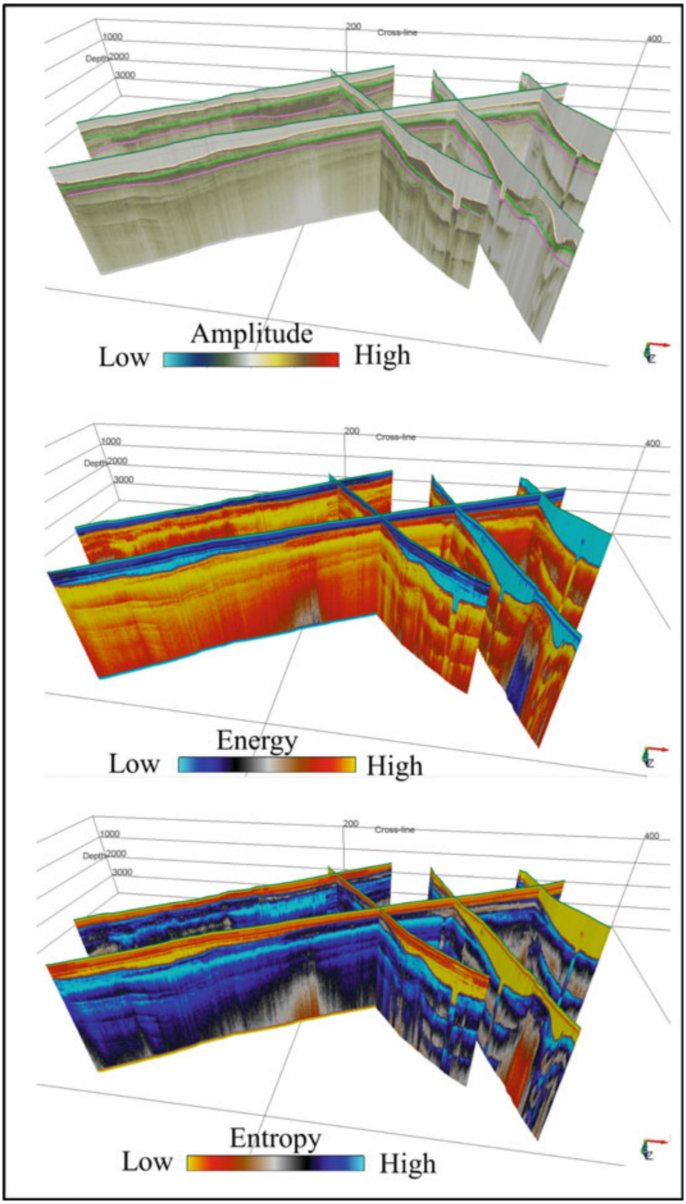

Fig. 7 Processed seismic data (top image) and its texture attributes, energy (middle image) and entropy (below image). Wheat, green, and pink lines are interpreted as seabed, top, and bottom of Holocene layer, respectively

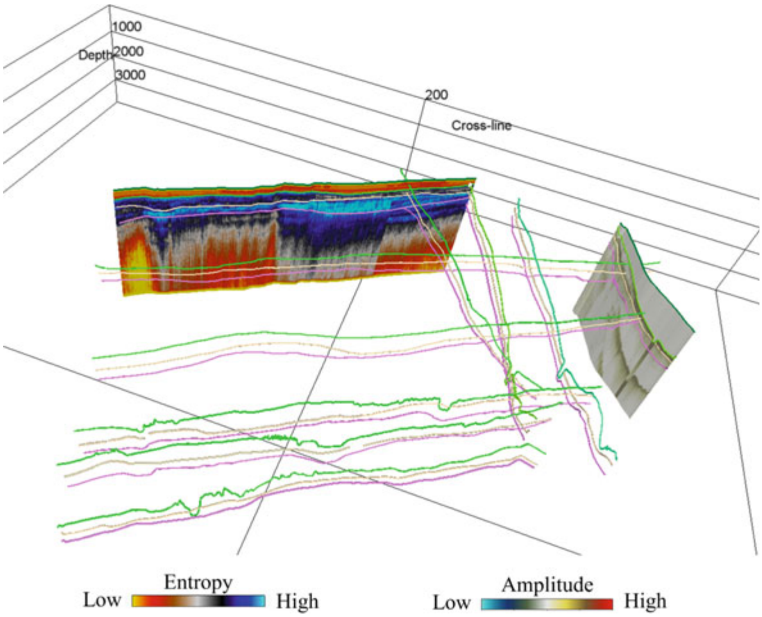

Fig. 8 Representation of all 2D interpreted seismic boundary. Processed seismic data and its textural attribute, entropy. Green, wheat color, and pink lines are interpreted as seabed, top and bottom of Holocene layer, respectively

Figs. 7 and 8). The boundaries between Holocene and Pleistocene layers are hardly seen through the processed seismic data but visible in their attributes helping its interpretation in different seismic profiles.

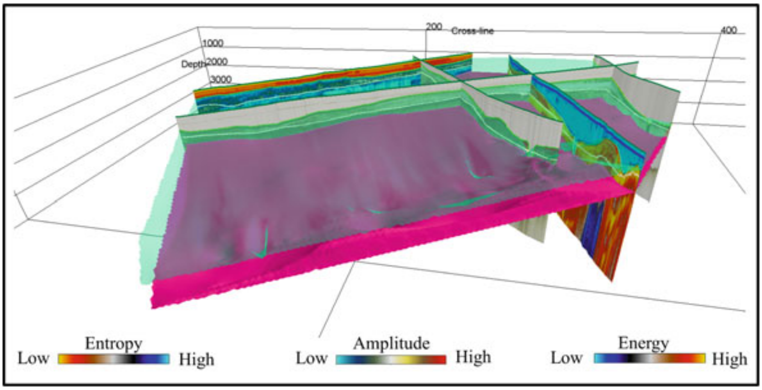

Fig. 9 3D seabed and Bottom Holocene made by 10 seismic profiles. Linear interpolation image with green surface for Seabed and pink one for Bottom Holocene

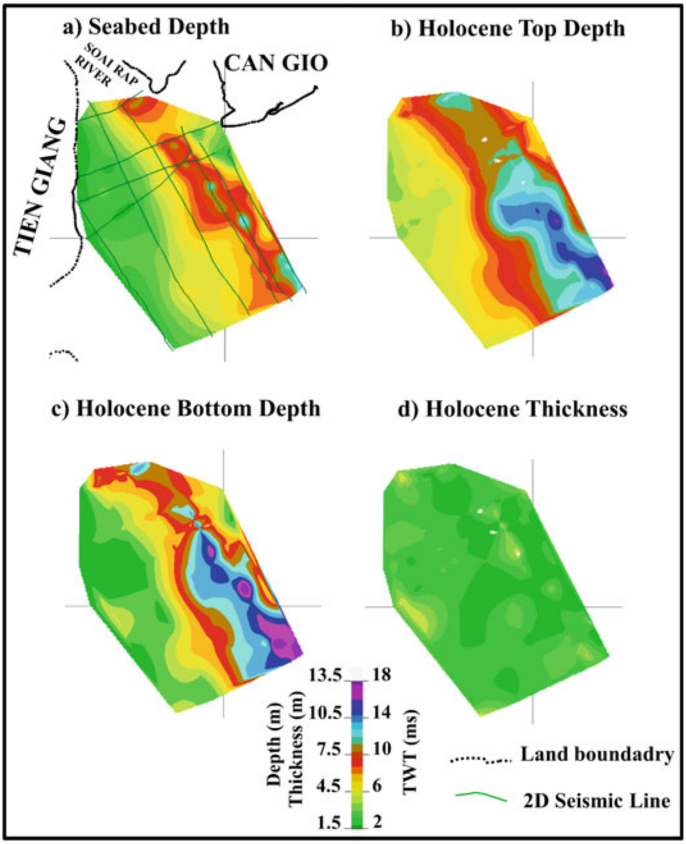

Fig. 10 3D seabed, top, bottom and thickness of Holocene layer made by ten seismic profiles. Holocene layer thickness can range from 1.5 m to around 4.5 m

Thickness of the Holocene layer can be calculated from the zone bounded by two 3D top and bottom surfaces. We have used propagation velocities as 1500 m/s and 1550 m/s for sea water and underground sediments, respectively [2] to convert two-way travel time (TWT) to depth. Note that multiple noise can interfere interpretation of the two 3D horizons. We have recognized seismic multiples by checking their travel time as double or triple of the original seismic events (See Fig. 7).

In the Fig. 10, 3D surfaces of seabed, the top, bottom, and thickness of Holocene layer are illustrated. There is distinguished river channel flowing northeast. The channel looks like to divide the interest area in to three different sub-areas with different depths in seabed, or top and bottom of Holocene layer. Figure 11 also shows a clear 3D visualization of the channel as seen as the red stripe.

According to the drill holes information [4] and the seismic interpretation result, we can determine three layers as follow:

(i) the first layer having mud, silk clay, sand, organic matter from Present time,

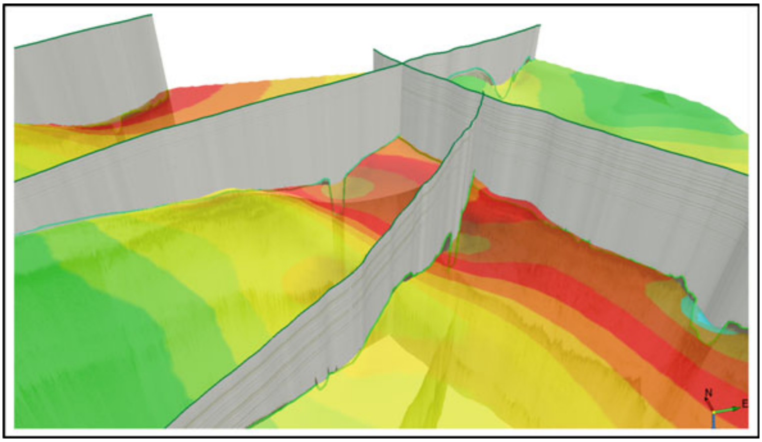

Fig. 11 3D view of small the Soai Rap river channel

(ii) the Holocene layer having clay sediment, and
(iii) the hard clay Pleistocene matters.

5 Conclusion

3D image of seabed and sedimentation in Soai Rap River fork can be presented using interpretation of 2D high-resolution seismic data. Suitable interpolation of different 2D boundaries which express zones of contrast of acoustic impedance can bring the 3D visualization come true with the help of useful professional software Matlab and OpendTect. Better interpreting the boundaries needs combination of different textural seismic attributes rather than just utilizing only the seismic processed data itself. Great match between seismic results and drill hole information as lithology can prove existence of Holocene layer and Pleistocene matters which helps to government officials in deepening the riverbed and canals for large ship transportation, especially, in Can Gio, Ho Chi Minh city. The distinguished Soai Rap channel appears in the seismic data can prove the fact that the high-resolution seismic data can detect small but meaningful geology features (Fig. 12).

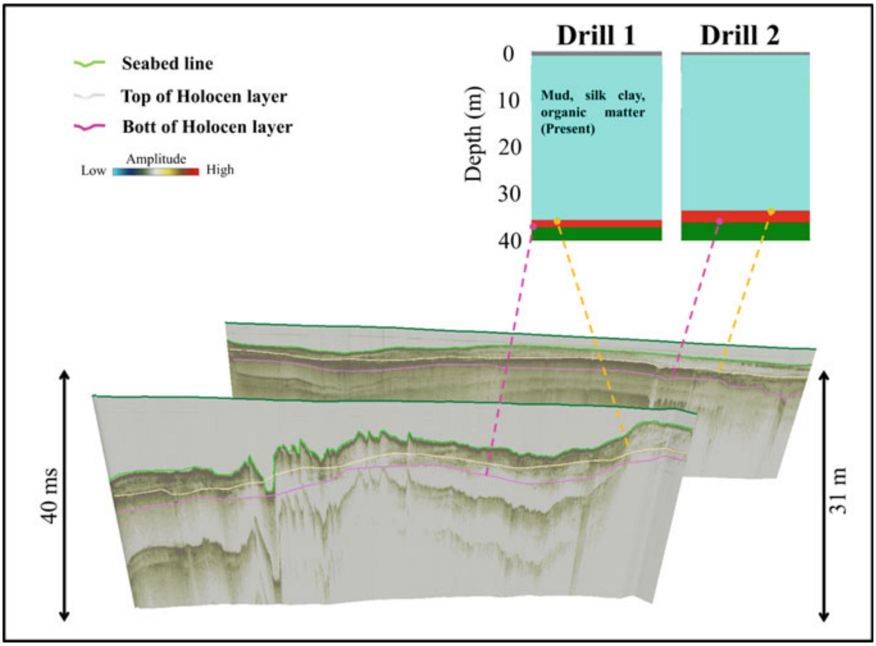

Fig. 12 Representations of two drill holes [4] with their two nearby seismic data profiles

Acknowledgements This research is funded by Vietnam National University Ho Chi Minh City (VNU-HCM) under grant number C2022-18-17. We would like to thank Mr. Nguyen Quang Dung for his help.

Conflicts of Interest The authors declare no conflict of interest.

Author Contribution All the authors contributed to the data analysis, interpretation, and manuscript. C.V.A.L mainly wrote the manuscript.

References

1. Ianniruberto, M., Campos, J.E., Araújo, V.: Application of shallow seismic profiling to study riverbed architectural facies: A case study of the Tocantins river (Pará-Brazil). An. Acad. Bras. Ciênc. **84**, 645–654 (2012)
2. Bui Viet, D., Stattegger, K., Unverricht, D., Van Phung, P., Nguyen Trung, T.: Late Pleistocene-Holocene seismic stratigraphy of the Southeast Vietnam Shelf. Global Planet. Change **110**, 156–169 (2013)
3. Novak, B., Björck, S.: Late Pleistocene–early Holocene fluvial facies and depositional processes in the Fehmarn Belt, between Germany and Denmark, revealed by high-resolution seismic and lithofacies analysis. Sedimentology **49**, 451–465 (2002)
4. Le, C.V.A., Duong, M.B., Kieu, T.D.: High–resolution seismic reflection survey of Holocene Sediment distribution at Thi Vai River, Ho Chi Minh City, Vietnam. Lecture Notes in Civil Engineering, vol. 2, pp. 290–304. Springer (2020)

5. Le, C.V.A., Harris, B.D., Pethick, A.M.: New perspectives on solid earth geology from seismic texture to cooperative inversion. Sci. Rep. **9**, 14737 (2019)
6. https://tuoitre.vn/luong-soai-rap-chinh-thuc-cho-tau-bien-30-000-tan-ve-tp-hcm-long-an-20200826115103097.htm
7. https://www.bandovn.vn/vi/page/mau-ban-do-hanh-chinh-nuoc-cong-hoa-xa-hoi-chu-nghia-viet-nam-181
8. David, F., Meziane, T., Tran-Thi, N.-T., Van, V.T., Thanh-Nho, N., Taillardat, P., Marchand, C.: Carbon biogeochemistry and CO 2 emissions in a human impacted and mangrove dominated tropical estuary (Can Gio, Vietnam). Biogeochem. **138**, 261–275 (2018)
9. Fujimoto, K., Umitsu, M., Nguyen, V.L., Ta, T.K.O., Kawase, K., Huynh, D.H., Nakamura, T.: Geomorphological evolution and mangrove habitat dynamics related to Holocene sea-level changes in the northern Mekong river delta and the Dong Nai river delta, southern Vietnam. In: Paul E. Schmidt (ed.) River Deltas: types, structures and ecology. Nova Science Publishers, Inc. (2011)
10. Bui, V.T., Huynh, T.T., Le, T.N.D., Ly, H.M., Le, P.T.: Monitoring and predicting the shoreline change in Can Gio area in condition of the sea level rise. Sci. Tech. Development J. **17**, 45–53 (2014)
11. Le, X.T., Vo, Q., Reyns, J., Pham, V.S., Tran, A.D., Dang, T.D., Roelvink, D.: Sediment transport and morphodynamical modeling on the estuaries and coastal zone of the Vietnamese Mekong Delta. Cont. Shelf Res. **186**, 64–76 (2019)
12. Stattegger, K., Tjallingii, R., Saito, Y., Michelli, M., Thanh, N.T., Wetzel, A.: Mid to late Holocene sea-level reconstruction of Southeast Vietnam using beachrock and beach-ridge deposits. Global Planet. Change **110**, 214–222 (2013)
13. Thoang, T., Giao, P.: Subsurface characterization and prediction of land subsidence for HCM City, Vietnam. Eng. Geol. **199**, 107–124 (2015)
14. Ta, T.K.O., Nguyen, V.L., Tateishi, M., Kobayashi, I., Tanabe, S., Saito, Y.: Holocene delta evolution and sediment discharge of the Mekong River, southern Vietnam. Quatern. Sci. Rev. **21**, 1807–1819 (2002)
15. Ta, T.K.O., Nguyen, V.L., Tateishi, M., Kobayashi, I., Saito, Y.: Holocene delta evolution and depositional models of the Mekong River Delta, southern Vietnam. River Deltas–Concepts, Models, and Examples, vol. 83. SEPM (Society for Sedimentary Geology) (2005)
16. Ta, T.K.O., Nguyen, V.L., Tateishi, M., Kobayashi, I., Saito, Y.: Sedimentary facies, diatom and foraminifer assemblages in a late Pleistocene-Holocene incised-valley sequence from the Mekong River Delta, Bentre Province, Southern Vietnam: the BT2 core. J. Asian Earth Sci. **20**, 83–94 (2001)
17. Nguyen, V.L., Ta, T.K.O., Saito, Y.: Early Holocene initiation of the Mekong River delta, Vietnam, and the response to Holocene sea-level changes detected from DT1 core analyses. Sed. Geol. **230**, 146–155 (2010)
18. Kitazawa, T.: Pleistocene macrotidal tide-dominated estuary–delta succession, along the Dong Nai River, southern Vietnam. Sed. Geol. **194**, 115–140 (2007)
19. Kitazawa, T., Nakagawa, T., Hashimoto, T., Tateishi, M.: Stratigraphy and optically stimulated luminescence (OSL) dating of a Quaternary sequence along the Dong Nai River, southern Vietnam. J. Asian Earth Sci. **27**, 788–804 (2006)
20. Yutsis, V., Krivosheya, K., Levchenko, O., Lowag, J., de León Gómez, H., Ponce, A.T.: Bottom topography, recent sedimentation and water volume of the Cerro Prieto Dam. NE Mexico. Geofísica internacional **53**, 27–38 (2014)
21. Aiello, G., Di Fiore, V., Marsella, E., Passaro, S.: High resolution seismic data coupled to Multibeam bathymetry of Stromboli island collected in the frame of the Stromboli geophysical experiment: implications with the marine geophysics and volcanology of the Aeolian Arc volcanic complex (Sicily, Southern Tyrrhenian sea, Italy). Springerplus **3**, 1–27 (2014)
22. https://www.edgetech.com/edgetech-introduces-new-portable-sub-bottom-profiling-system/
23. https://www.edgetech.com/resource-center/
24. VectorStock: Ship Image
25. EdgeTech: JSF Data File Description (2016)

26. https://www.sandmeier-geo.de/reflexw.html
27. dGB Earth Sciences: OpendTect dGB Plugins User Documentation version 4.6. (2015)
28. Yilmaz, O.: Seismic data analysis: processing, inversion, and interpretation of seismic data. Soc. Explor. Geophys., United States of America (2001)
29. Le, C.V.A., Harris, B.D., Pethick, A.M., Takam Takougang, E.M., Howe, B.: Semiautomatic and automatic cooperative inversion of seismic and magnetotelluric data. Surveys Geophys. **37**, 845–896 (2016)
30. Chopra, S., Marfurt, K.J.: Seismic attributes for prospect identification and reservoir characterization. Tulsa, Okla. (8801 South Yale St., Tulsa OK 74137–3175): Society of Exploration Geophysicists, United States of America (2007)
31. http://www.fp.ucalgary.ca/mhallbey/tutorial.htm
32. Haralick, R.M., Shanmugam, K., Dinstein, I.: Textural features for image classification. IEEE Trans. Syst. Man, Cybernetics SMC-3, 610–621 (1973)
33. https://www.mathworks.com/help/matlab/ref/scatteredinterpolant.html